JOURNAL OF MATERIALS SCIENCE 3 (1968) 629–634

The Strength of Two-Phase Ceramic/Glass Materials

R. W. DAVIDGE, T. J. GREEN
Materials Development Division, United Kingdom Atomic Energy Authority Research Group, Atomic Energy Research Establishment, Harwell, Berks, UK

Received 13 May 1968

The strengths of various glasses, with a range of expansion coefficients, containing 10 vol % thoria spheres, of diameter 50 to 700μm, have been measured. Stresses occur around the spheres, due to differences in the expansion coefficients of the glass and the spheres, on cooling from the fabrication temperature. Stress magnification occurs near the spheres, due to differences in elastic properties, in the presence of an applied stress. When the expansion coefficient of the sphere is greater than that of the glass, circumferential cracks form around the spheres but only when the sphere diameter is greater than a critical value. An approximate value for the critical diameter may be obtained by an energy balance criterion. Cracks may form around spheres smaller than the critical diameter under application of applied stress at stresses below the macroscopic fracture stress. In these cases the strength is governed by a Griffith relationship with the crack size equal to the sphere diameter. When the expansion coefficients of the spheres and glass are similar, the strength of the glass is reduced only when large spheres ($\lesssim$300 μm diameter) are present. When the expansion coefficient of the spheres is less than that of the glass, linking radial cracks form between the spheres and the material has very low strength.

1. Introduction

Numerous ceramic materials of commercial importance comprise a crystalline phase embedded in a glassy matrix. These include debased aluminas (>85% Al_2O_3 in glass) and electrical porcelains (~25% SiO_2 in glass). The factors controlling the strength of such materials are not fully understood. Because of this a number of studies have been performed on "model" systems, generally particles of crystalline ceramic (often in spherical form) in various glassy matrixes. The important strength-controlling factors to emerge are [1-5]: (i) the expansion coefficients of the two phases; (ii) the volume-fraction of the crystalline phase; (iii) the particle-size of the crystalline phase; (iv) the elastic properties of the two phases.

In ceramic/glass composites only the first three factors can be varied significantly. Of these, only the first two have received detailed attention. The current investigation is concerned with the effects of particle-size. Thoria was chosen as the ceramic since highly perfect spheres, with a wide range of diameters and of near theoretical density, were readily available.

The objective of this work is limited to a study of the effects on mechanical properties of stresses around the particles. Composites containing 10 vol% of spheres are used so that sphere-sphere interactions are relatively unimportant. There are two types of sphere-matrix interaction of relevance: those formed during cooling of the composite after fabrication due to differences in thermal expansion coefficients, and, stress magnification effects under the influence of an applied external stress due to differences in elastic properties. To separate these two factors, four sets of composites were made with glasses of different expansion coefficient.

2. Stresses Around Particles

2.1. Stresses due to Differences in Thermal Expansion Coefficient

The theory concerning the stress system around

particles in an isotropic medium is well established. Because the expansion coefficients of the two phases are generally different, stresses are set up within and around the particles as the body cools down from the fabrication temperature. A spherical particle will be subjected to a pressure P (equivalent to radial and tangential stresses of $-P$) and the matrix to radial and tangential stresses of $-PR^3/r^3$ and $+PR^3/2r^3$ respectively* where R is the particle radius and r the distance from a point in the matrix to the centre of the particle. Ideally these equations hold only for the case of a single particle in an infinite isotropic matrix, but they represent a satisfactory approximation at low particle concentrations. Weyl [6] and Selsing [7] have shown that

$$P = \frac{\Delta\alpha\,\Delta T}{(1+\nu_1)/2E_1 + (1-2\nu_2)/E_2}, \qquad (1)$$

where $\Delta\alpha$ is the difference in the two expansion coefficients, ΔT is the cooling range over which the matrix plasticity is negligible (taken to be from the annealing point temperature to ambient) and $\nu_{1,2}$, $E_{1,2}$ the Poisson's ratio and Young's modulus of the matrix and particle respectively. The pressures P for the four systems used are included in table I. The values $\nu_1 = 0.20$, $\nu_2 = 0.275$, $E_1 = 7 \times 10^{11}$ dyn/cm^2 and $E_2 = 2.5 \times 10^{12}$ dyn/cm^2 were used in equation 1.

Equation 1 shows that the magnitude of the stresses is independent of particle-size. Experimentally it is observed that, for a particular system, cracking occurs only around particles greater than a critical size [1]. The formation of cracks must depend therefore on both the stress magnitude and the particle-size.

The nature of the cracking, if it occurs, depends on whether the particles contract more or less than the matrix during cooling. In the former case P is negative and cracking is circumferential around the particles. In the latter case P is positive and cracking occurs radially from the particles; this is more deleterious to strength because cracks from individual particles can easily link up. An excellent statement of these effects is given in the paper by Binns [1].

2.2. Stresses due to Differences in Elastic Properties

This case has been considered by Hasselman and Fulrath [3]. The solutions of Goodier [8] for the stress concentrations around circular inclusions in a two-dimensional plate were used, since these gave the best available approximation to the experimental conditions. Stresses occur only in the presence of an applied stress and the important point is that the applied stresses become magnified in the vicinity of the sphere. In a bend test, where the applied stress can be considered as a uniaxial tensile stress, the region of significant stress magnification is limited to a zone around the direction of the tensile stress. This is illustrated in fig. 1. The maximum stress

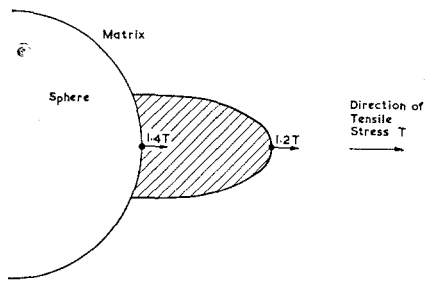

Figure 1 Stress concentrations due to differences in elastic properties.

concentration is 1.4 times and occurs at a point on the surface of the sphere. The hatched area shows the region subjected to a stress concentration of more than 1.2 times. Again the magnitude of the stresses is independent of the sphere diameter.

3. Experimental

3.1. Materials

Four glasses were used and relevant property data are given in table I. The values for the thermal expansion coefficients usually quoted are for the temperature range from ambient up to about 300 to 350° C. However, the expansion coefficient of glasses increases steadily with temperature until just above the annealing point. An example for G4, is shown in fig. 2 [9]. At the annealing point it takes about 15 min to relieve the strains in a glass. The appropriate expansion coefficient to consider with respect to the current fabrication procedure (see below) is therefore from 20° C to the annealing point.

The thoria spheres were prepared by a sol-gel method [10]. The gel spheres were dried at 80° C and calcined to dense (98% theoretical density) spheres of thoria at 1150° C for 2 h. These

*Positive pressures are compressive and positive stresses are tensile: and vice versa.

TABLE I Property data for glasses and thoria.

Material	Density (g/cm^3)	Softening point (viscosity $10^{7.6}$ poise) (°C)	Annealing point (viscosity 10^{13} poise) (°C)	Effective cooling range, ΔT (°C)	Mean expansion coefficient (20° C to annealing point) (10^{-6} °C^{-1})	Expansion coefficient difference, $\Delta\alpha$ (10^{-6}°C^{-1})	$\Delta \alpha \Delta T$ (10^{-3})	P (equation 1) (10^8 dyn/cm^2)
G1 Corning 7740 Pyrex	2.23	820	565	545	3.6	−5.1	−2.78	−26.7
G2 Plowden & Thompson Kodial	2.27	750	520	500	5.4	−3.3	−1.65	−15.9
G3 GEC GS72 Borosilicate	2.46	765	600	580	7.9	−0.8	−0.46	− 4.5
G4 GEC X8 Soda-lime	2.49	715	530	510	10.5	+1.8	+0.92	+ 8.8
– Sol-gel ThO_2 spheres	9.90	—	—	—	8.7 (0-500° C)	—	—	—

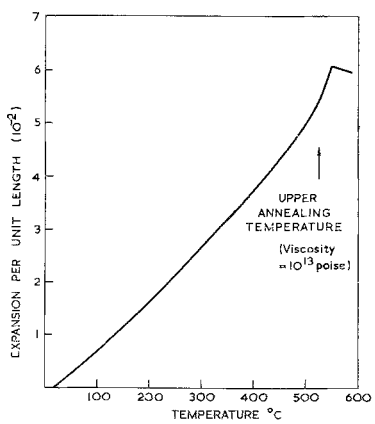

Figure 2 Thermal expansion curve for glass G4 [9].

resultant spheres were sieved into sixteen grades in the diameter range 45 to 710 μm. In each range the total spread of sphere diameters was $\pm 10\%$ of the mean diameter.

3.2. Sample Preparation

The glasses were crushed to a fine powder in a percussion mortar and pestle. The powdered glass was sieved into various size ranges < 250 μm. Metal contamination from the mortar and pestle was removed with a magnet.

Composites containing 10 vol % of thoria were prepared by wet-mixing each grade of thoria with glass powder of finer size in isopropanol, and vacuum hot-pressing in a 3 cm diameter graphite die for 30 min at a temperature 20° C below the softening point of the glass and at a pressure of 1000 psi (1.0 psi = 1.0 lb/in^2 = 7.0×10^{-2} kg/cm^2). The cooling rate in the region of the annealing point was ~5° C/min. The cylindrical samples approximately 1 cm thick were cut into specimens for fracture strength measurements using a precision diamond saw. No particular care was taken during the cutting operation except that all specimens were cut under standard conditions. This treatment inevitably introduces surface flaws into the specimens but it assumed that the amount of damage is roughly constant.

3.3. Measurement of Fracture Strength

Specimens were ~15 mm long and 4 mm square cross-section. These were tested in three-point bending with a 10 mm span in an Instron machine operating with a cross-head speed of 0.05 cm/min. At least six specimens were tested from each compact. The average spread of strength values was $\pm 15\%$ from the mean strength.

4. Results

4.1. Microexamination

In glasses G1 and G2 circumferential cracks occur around the thoria spheres, fig. 3a. Although the majority of cracks lie away from the sphere-glass interface, the central portions of many cracks do coincide with, or pass very close to, the interface. This view is reinforced by examination of specimens in transmitted light, and suggests that cracks originate at the interface and then spread out into the glass.

The frequency of cracking depends on the sphere diameter. In G1 no cracks were observed around spheres $\leqslant 59$ μm diameter whereas at least 25% of spheres $\geqslant 83$ μm diameter had cracks around them. In G2 no cracks were

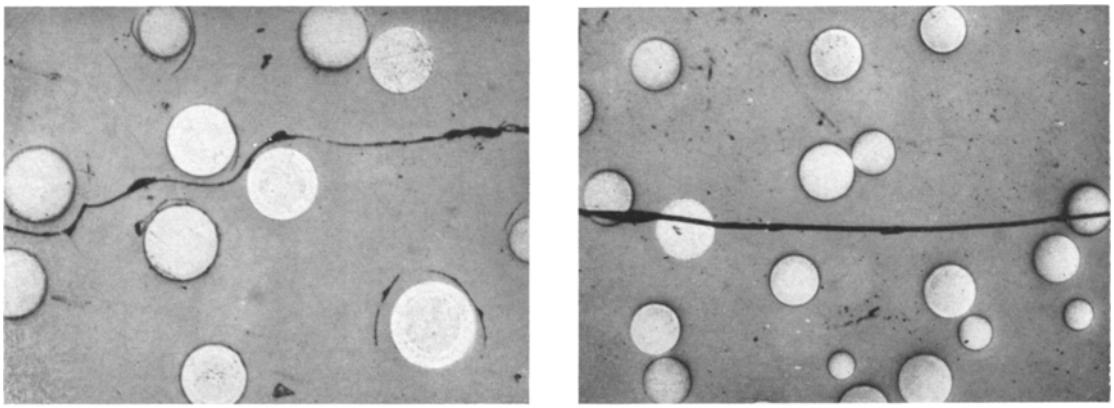

(a) (b)

Figure 3 Fracture paths in glasses containing thoria spheres 125 to 150 μm dia. (a) G1 ($\times$ 64); (b) G4 ($\times$ 43).

observed around spheres $\leqslant$ 195 μm diameter, and significant cracking ($>$ 10% frequency) was found around spheres $>$ 275 μm diameter.

No cracking occurred in G3. All compacts of G4 broke into several pieces on removal from the pressing die and specimens with the larger spheres showed a linked network of cracking. The cracks passed through the spheres and into the glass from a radial direction.

Macroscopic fracture paths, in externally stressed specimens, passed round the spheres in G1 and G2, fig. 3a, and through the spheres in G3 and G4, fig. 3b.

Microexamination of the surface region opposite the central load point during the application of an applied stress revealed little change in the crack system of most specimens, until catastrophic failure at the fracture stress. However, in G2 containing spheres of 100 to 200 μm diameter circumferential cracks were sometimes observed to develop around the spheres at stresses below the fracture stress. The critical flaw is thus not necessarily in the as-fabricated specimen, but may develop under the combined action of internal and applied stresses.

Only in a few isolated cases, with the larger spheres, did spheres "fall out" of the matrix. It is considered, therefore, that there is good bonding between sphere and matrix.

4.2. Strength Measurements

Results for G1, G2, and G3 are given in fig. 4. There is no significant difference in the results for G1 and G2, but for a given sphere diameter the strength of G3 is the greatest. Spheres $<$ 300 μm diameter in G3 produce little

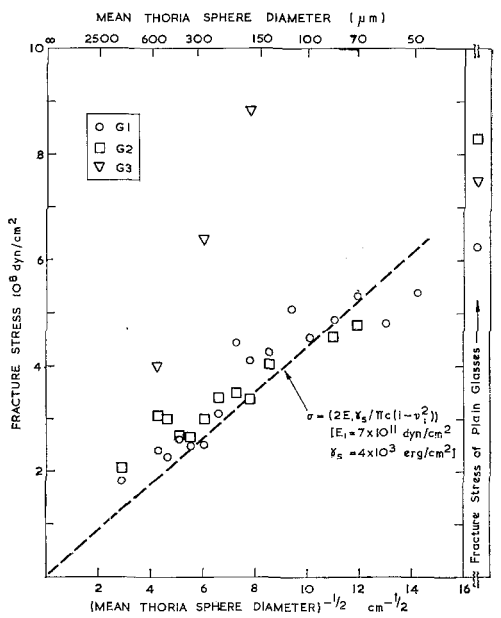

Figure 4 Strength-sphere size data for glass G1, G2, and G3.

reduction in strength, and may in fact lead to a small increase. The strengths of G1 and G2 fall steadily with increasing sphere diameter.

5. Discussion

5.1. The Criterion for Circumferential Cracking in the Absence of Applied Stress

The production of a circumferential crack, in the case where the particle has a higher thermal expansion coefficient than that of the matrix, requires the presence of some flaw near the

particle and a supply of energy for the flaw to grow. It is obviously not sufficient that the macroscopic strength be reached because the stresses at the particle surface in both G1 and G2 exceed the macroscopic strength (cf table I and fig. 4), yet cracking is found only round particles above a particular size. Energy for a growing flaw is provided by the elastic stored energy in the particle and in the surrounding matrix. The rate of energy release to the flaw as it grows is difficult to determine, but a high proportion of the stored energy can be released if the crack grows completely round the sphere.

The total stored energy per unit volume may be calculated. The elastic energy, U, in an element of material subjected to orthogonal tensile (or compressive) stresses P_1, P_2 and P_3 is [11]

$$U = \frac{1}{2E}\{(1+\nu)(P_1^2 + P_2^2 + P_3^2) - \nu(P_1 + P_2 + P_3)^2\}$$

The energy in the matrix, using $-P_1 = +2P_2 = +2P_3 = PR^3/r^3$, is thus

$$U_1 = \int_R^\infty \frac{(1+\nu_1)}{2E_1} \cdot \frac{3}{2} P^2 \frac{R^6}{r^6} \cdot 4\pi r^2 \, dr = \frac{3P^2(1+\nu_1)}{4E_1} \cdot \frac{4}{3}\pi R^3 \quad (2)$$

Note that the matrix strain energy is highly localised around the particle: seven-eighths of U_1 is included in the matrix volume from $r = R$ to $r = 2R$. The energy within the sphere is, using the information in 2.1,

$$U_2 = \frac{3P^2(1-2\nu_2)}{2E_2} \cdot \frac{4}{3}\pi R^3 \quad (3)$$

Summing equations 2 and 3 gives the total energy, U_T.

$$U_T = P^2\pi R^3 \left\{\frac{(1+\nu_1)}{E_1} + \frac{2(1-2\nu_2)}{E_2}\right\} \quad (4)$$

A necessary, but not necessarily sufficient, condition for crack formation is that the energy to create a new surface, U_S, cannot exceed U_T, i.e.

$$U_T \geqslant U_S \quad (5)$$

$U_S = \gamma_S A$ where γ_S is the effective surface energy of the matrix, which will be taken as 4×10^3 erg/cm^2 [2, 12], and A is the area of surface produced. Experimentally it is observed that, when cracking occurs, a roughly hemispherical crack forms round each sphere; A will thus be taken as $\sim 4\pi R^2$ (taking account of the two surfaces of the crack). So,

$$U_S = 4\pi R^2 \gamma_S . \quad (6)$$

It is assumed further that the formation of the hemispherical crack liberates half of U_T. The energy available is proportional to R^3 whereas the energy absorbed in cracking is proportional to R^2. Combining equations 4, 5, and 6 thus gives for the critical radius R_c

$$R_c \geqslant 8\gamma_S / \{P^2[(1+\nu_1)/E_1 + 2(1-2\nu_2)/E_2]\} \quad (7)$$

For G1, G2 and G3, substituting values of P from table I in equation 7, one obtains values of R_c, respectively 22, 62, and 770 μm. The observed values of R_c for G1 and G2 are $\sim$35 and 115 μm, i.e. somewhat greater than the calculated values, indicating that the controlling step in crack-formation may be that of nucleation. Nevertheless, the observed and calculated values for R_c are close enough to justify the use of equation 7 to indicate approximate values of R_c.

5.2. Strength versus Particle-Size

For the materials studied here, the strengths of the plain glasses are superior or equal to those of the composites. The critical flaw sizes for the plain glasses, according to the Griffith equation, vary from $\sim$50 μm (G1) to 30 μm (G2). The effect of spheres $\geqslant$ 50 μm is thus to introduce flaws larger than the inherent flaws, and so reduce the strength.

When circumferential cracking occurs round the spheres, as in G1, the strength should follow a Griffith relationship with a flaw size of approximately the sphere diameter. This should hold also for G2, since cracks of sphere diameter dimensions form at stresses below the fracture stress in the case where no cracks occur during fabrication. The expected relationship is shown in fig. 4, and this agrees closely with the data for G1 and G2. The effect of possible stress concentrations due to differences in elastic properties will be small in G1 and G2 because the spheres are effectively isolated from the matrix by the cracks. In G3 there is only a reduction in strength when large spheres are present. In this system any strength reduction depends on the regions of stress concentration around the spheres, fig. 1. It is not possible to predict quantitative behaviour because this is controlled by the size and distribution of Griffith flaws with respect to the regions of stress concentration. This approach is the essence of the qualitative description of the

effect of porosity on the strength of glass by Hasselman and Fulrath [3].

5.3. General Implications

An important conclusion of the present study is that one cannot suppose, as has been done previously [13], that the macroscopic fracture stress is reduced by an amount equal to the internal stress. In some cases the internal stress may be several times larger than the macroscopic fracture stress. Instead it is more meaningful to consider the effects of internal stress on an energy basis as done above. Large particles of second phase therefore are more deleterious to strength than small particles. The strongest material, other things being equal, is thus likely to have the finest particle-size.

When the expansion coefficients of the two phases are matched, there is no strength reduction except when large spheres are present. Indeed, Hasselman and Fulrath [2] showed that in such systems (glass/alumina $\leqslant 60$ μm diameter) the strength increased when the mean distance between spheres was < 50 μm (the inherent flaw size) and suggested that the intersphere distance was closely related to the Griffith flaw size. The maximum density of alumina spheres used was 47.5% which corresponded to a minimum flaw size of ~ 14 μm.

It would, however, be dangerous to extrapolate these ideas, to say, high alumina bodies containing $< 15\%$ of glassy phase where the distance between alumina particles may be only a few μm. In the ceramic sphere/glass model systems the glass phase is definitely the weakest link in the structure compared with the ceramic/glass interface or the ceramic particle itself. In high alumina bodies it is necessary first to identify the source of fracture before any interpretation may be made.

6. Conclusions

(i) The effects of differences in expansion coefficient and elastic constants on the strength of four glasses containing thoria spheres of various sizes have been studied. Both these factors lead to a reduction in strength but only for spheres larger than a given size. The first effect is the more important.

(ii) When the expansion coefficient of the spheres is greater than that of the glass, the weakening effect is due to the introduction of Griffith cracks, of length similar to the sphere diameter, that are larger than the inherent flaws in the glass (~ 50 μm).

(iii) In as-fabricated specimens, these cracks occur only around spheres of diameter larger than a critical diameter. This critical diameter can be estimated approximately from an energy balance criterion. Nevertheless, under the action of an applied stress, cracks may occur round spheres with a diameter smaller than critical at a stress lower than the macroscopic fracture stress. The absence of cracking in as-fabricated specimens cannot therefore be taken as an indication that the strength will not be reduced.

(iv) The situation where the expansion coefficient of the sphere is less than that of the matrix should be avoided, since this leads to very poor mechanical properties. In the design of materials with the highest strength, of the type discussed in this paper, it is recommended that the particle and matrix expansion coefficients be matched, and that the particle size be as small as possible.

Acknowledgements

Thanks are due to Dr F. J. P. Clarke for stimulating discussions, and to Dr C. J. Hardy for supplying the thoria spheres.

References

1. D. B. BINNS, "Science of Ceramics", Vol. 1, edited by G. H. Stewart (Academic Press, London, 1962) p. 315.
2. D. P. H. HASSELMAN and R. M. FULRATH, *J. Amer. Ceram. Soc.* **49** (1966) 68.
3. *Idem, ibid* **50** (1967) 399.
4. R. L. BERTOLOTTI and R. M. FULRATH, *ibid* p. 558.
5. W. J. FREY and J. D. MACKENZIE, *J. Materials Sci.* **2** (1967) 124.
6. D. WEYL, *Ber. deut. keram. Ges.* **36** (1959) 319.
7. J. SELSING, *J. Amer. Ceram. Soc.* **44** (1961) 419.
8. J. N. GOODIER, *J. Appl. Mech.* **1** (1933) 39.
9. "Glass" (GEC, 1959) p. 4.
10. J. M. FLETCHER and C. J. HARDY, *Chemistry and Industry* **76** (1968) 48.
11. J. PRESCOTT, "Applied Elasticity" (Longmans, 1924) p. 188.
12. R. W. DAVIDGE and G. TAPPIN, *J. Materials Sci.* **3** (1968) 165.
13. R. L. COBLE "Ceramic Fabrication Processes", edited by W. D. Kingery (Technology Press of MIT, 1958) p. 213.